

# Radiation-induced conductivity in polystyrene at extremely low (79 K) temperature

Cite as: J. Appl. Phys. **132**, 135105 (2022); <https://doi.org/10.1063/5.0106159>

Submitted: 27 June 2022 • Accepted: 03 September 2022 • Published Online: 03 October 2022

 Andrey Tyutnev,  Vladimir Saenko,  Ilshat Mullakhmetov, et al.



View Online



Export Citation



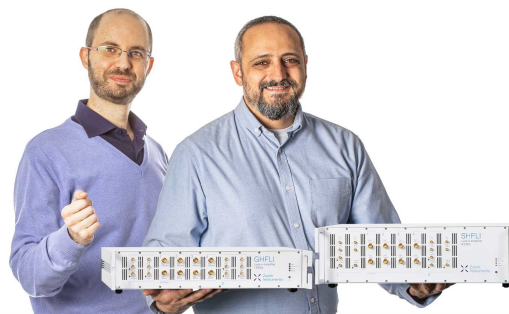
CrossMark

Webinar

Meet the Lock-in Amplifiers  
that measure microwaves

Oct. 6th – Register now

 Zurich  
Instruments



# Radiation-induced conductivity in polystyrene at extremely low (79 K) temperature

Cite as: J. Appl. Phys. **132**, 135105 (2022); doi: [10.1063/5.0106159](https://doi.org/10.1063/5.0106159)

Submitted: 27 June 2022 · Accepted: 3 September 2022 ·

Published Online: 3 October 2022



View Online



Export Citation



CrossMark

Andrey Tyutnev,<sup>a)</sup> Vladimir Saenko,<sup>b)</sup> Ilshat Mullakhmetov, and Andrey Abrameshin

## AFFILIATIONS

National Research University Higher School of Economics, 20 Miasnitskaya Ulitsa, Moscow 101000, Russia

<sup>a)</sup>E-mail: [aptyutnev@yandex.ru](mailto:aptyutnev@yandex.ru)

<sup>b)</sup>Author to whom correspondence should be addressed: [saenko19@gmail.com](mailto:saenko19@gmail.com)

## ABSTRACT

Radiation-induced conductivity (RIC) of polystyrene has been studied experimentally and numerically in a broad time range from milliseconds to seconds at 79 K, which seems to have been done for the first time. It has been established that the hole dispersive transport is still operative but unlike the room temperature behavior it features an extremely small frequency factor ( $4 \times 10^3 \text{ s}^{-1}$ ) and accordingly low dispersion parameter (0.09). It has been shown that prompt conductivity per unit dose rate does not depend on temperature (290 or 79 K) and is equal to  $K_p = 3.5 \times 10^{-15} \Omega^{-1} \text{ m}^{-1} \text{ Gy}^{-1} \text{ s}$  ( $\pm 20\%$ ) at  $4 \times 10^7 \text{ V/m}$ . At 79 K, current–voltage characteristics of both prompt and delayed components are close enough and non-linear. Due to the contribution of the thermalized charge carriers, the RIC even at 79 K can be satisfactorily described by the semi-empirical Rose–Fowler–Vaisberg model based on the quasi-band multiple trapping mechanism just as it happens at room temperature.

Published under an exclusive license by AIP Publishing. <https://doi.org/10.1063/5.0106159>

## I. INTRODUCTION

Spacecraft charging continues to be the most important factor causing spacecraft electronics failure on geosynchronous or highly elliptical orbits.<sup>1</sup> The main approach to eliminate this negative factor consists in making a reasonable choice of insulating materials (polymers as a rule), which exclude initiating of electrostatic discharges (ESDs). Insulators resistance to ESD formation increases with rising of their total conductivity [the sum of the dark and radiation-induced conductivity (RIC)]. Both conductivities decrease as temperature goes down. To be able to make a qualified selection of polymers for spacecraft application, one needs to develop experimental techniques for conductivity studies in polymers at low temperatures.

Polystyrene (PS) is currently often used as a model for the investigation of RIC in polymers. It is a typical weakly polar polymer with small AC dielectric losses featuring an extremely small dark conductivity. Under irradiation, it exhibits a highly dispersive hole transport. Its RIC at room temperature is sufficiently high thus securing an ESD free operation in the worst case of a non-penetrating monoenergetic electron irradiation of a polymer slab.

Nowadays, there exist a number of empirical criteria defining ESD resistance of spacecraft insulators. One relating to the case of a bulk electron accumulation defines a maximum electric field

$2 \times 10^7 \text{ V/m}$ , which surely excludes ESD in the bulk of a polymer. The maximum electric field under above irradiation conditions may be found using the formula suggested by Gross:<sup>2</sup>  $F_{\max} = j_e/\gamma_r$  where  $j_e$  is an electron current density normally falling on a polymer slab and  $\gamma_r$  is a polymer steady-state RIC. This formula seems to be rather simple, but the detailed analysis of  $\gamma_r$  shows that it depends on dose rate, irradiation time (absorbed dose), bulk electric field, and temperature in a most complicated way.<sup>3</sup> As a result, a correct assessment of the ESD resistance of a specified polymer requires carrying out a whole cycle of laboratory studies.

Extensive investigations of the RIC in PS subjected to pulsed or long-time irradiations at room and higher temperatures<sup>4,5</sup> have shown that the traditional Rose–Fowler–Vaisberg (RFV) model<sup>3,6</sup> describes successfully the existing experimental data with its parameters determined by fitting laboratory results. An important parameter, the so-called free ion yield  $G_{fi}$ , relating the experimentally used dose rate with the carrier generation rate appearing in the numerical calculations has also been obtained with an acceptable accuracy.<sup>5</sup> From an engineering point of view, the above problem has been adequately solved at least at room temperature.

Now, we intend to study the low temperature features of the RIC in PS in a broad range of irradiation times at an extremely low

temperature of 79 K believing that this way we are dealing with the phenomenon in its most severe manifestation. Under these conditions, the delayed component of the RIC that is the only legitimate object of the RFV model is expected to be almost lost on the background of the prevailing prompt component, whose origin could hardly be due to the thermalized carriers only. The contribution of hot electrons with energy of about several eV should not be overlooked.

Inevitably, at such low temperatures, one is bound to take into account the existence of geminate electron-hole pairs whose life increases sharply compared to a room temperature.<sup>7,8</sup> It is known that the RFV model neglects their contribution.

Hole transport in PS is strongly dispersive, in highly non-equilibrium condition, with the dispersion parameter  $\alpha = 0.35$  at room temperature so that the well-developed theory of the anomalous charge carrier transport may be applied for the data interpretation.<sup>4,5</sup> We plan to use it at low temperatures for interpreting experimental results and fulfilling numerical calculations to parameterize the RFV model in this case as well. Also, we would like to concern some ambiguities in the interpretation of the RIC prompt conductivity.

## II. EXPERIMENTAL

### A. Methodology

As in our previous experiments,<sup>4,5</sup> we used the capacitor-grade, biaxially stretched PS films (Styroflex, 20  $\mu\text{m}$  thick produced by NSW firm, FRG). Samples have been cut from the same band 100 mm wide with a shelf life of about 35 years which is still at our disposal. Specimens (40 mm in diameter) were supplied with evaporated 50 nm Al electrodes, 32 mm in diameter. We used only *fresh* samples for each long-time irradiation run. Experiments have been conducted at 79 K and most data refer to an electric field of  $4 \times 10^7$  V/m.

Like in Refs. 4 and 5, we used an ELA-50 electron gun as an irradiation source slightly modified to accommodate low temperature measurements (Fig. 1). Monoenergetic 50-keV electrons fall normally upon a polymer sample in a pulsed or long-time irradiation regime. A shutter 12 with an opening time of 0.08 s is used to set the beam current beforehand and manually control a continuous irradiation regime. For the beam current of 1 nA (1 mV/1 M $\Omega$ ) measured by the shutter, there would be a dose rate of 1.7 Gy/s in PS.<sup>9</sup> But due to the presence of the one-side metallized film 5  $\mu\text{m}$  thick 13 intended to reflect light from a hot electron source 1 away from a test sample 17, this dose rate decreases to 1.3 Gy/s. Beam collimator is 20 mm in diameter. Irradiation and measuring techniques are the same as in Ref. 4.

We employed a passive temperature control allowing the temperature of the sample holder and the Faraday cup 18 to reach a constant 79 K as registered by a copper-constantan thermocouple 16 in about 50 min. This is achieved by a combination of the heat-removing copper block 10 to the Dewar's vessel with liquid nitrogen (7,8) and a light reflector 13.

### B. General phenomenology

An experimentally measured quantity is the RIC current density  $j_r$ . The raw data were processed to separate the delayed

component  $j_{rd}$  from the total signal:  $j_{rd} = j_r - j_p$ , where  $j_p$  is the RIC prompt component.<sup>3,4</sup> In the case of the small-signal irradiation when an applied field is uniform and constant, it is useful to introduce the normalized quantities: conductivity  $\gamma_r = j_r/F_0$  and reduced conductivity  $K_r = \gamma_r/R_0$  separating delayed and prompt components (low indices for  $r$  being  $rd$  and  $p$ , respectively).

We are mainly interested in the delayed component that defines the transport properties of a polymer. Usually, the reduced prompt conductivity  $K_p$  is presumed to be a material parameter<sup>1</sup> and needs only once to be determined.

In the RFV model, an exponent  $\beta = d\lg j_{rd}/d\lg t$  stays constant during an irradiation time and in this case,  $\beta = \alpha$  (the dispersion parameter of the model). At a long-time irradiation driving the RIC into recombination-controlled regime, one observes a power-like dependence of the maximum RIC on the dose rate  $R_0$ ,

$$\gamma_{rm} \propto R_0^\Delta, \quad (1)$$

with  $\Delta = (1 + \alpha)^{-1}$ . The current decay in a rather broad time interval after the maximum still under irradiation is given by the following expression:

$$\gamma_{rd} \propto t^{-(1-\alpha)/2}, \quad (2)$$

as this has been first analytically established by Arkhipov and Rudenko<sup>10</sup> back in 1983.

### C. Experimental results

As expected, RIC at 79 K appreciably falls compared with that at room temperature (Figs. 2 and 3) for both pulsed and long-time irradiations including the recombination affected conditions in the last case. The total RIC (i.e.,  $\gamma_r$ ) decreases by about 40 times, while its delayed component diminishes by a factor of 200 as Fig. 2 shows for a decaying current after the pulse end. At the end of a 1-ms pulse,  $K_{rd}$  constitutes only about 1/5 of  $K_p$  (curve 2 in Fig. 2) reflecting the fact that delayed component is seen to be slowly rising during irradiation time contrary to what is observed for curve 1. It is seen that the initial part of the decaying  $\gamma_{rd}$  merges with that of the prompt component and its value immediately after the pulse end should be assessed as  $\gamma_{rd}(0) = \gamma_r(0) - \gamma_p$ , where the first term refers to the pulse end. Asymptotically,  $j_{rd}$  decays according to the law  $t^{-0.9}$ . As we will see later, these data allow determining the frequency factor of the RFV model.

Curve 2 in Fig. 3 serves mostly as auxiliary information in model parameterization. Vertical dashed line marks the time from which experimental results are free from methodological limitations such as RC time constant or shutter opening effects.<sup>4</sup> The earliest measured reduced current density on curve 2 ( $K_r = 5.6 \times 10^{-15} \Omega^{-1} \text{m}^{-1} \text{Gy}^{-1} \text{s}$ ) exceeds  $K_p$  by approximately 1.6 times (for the current maximum, this ratio is close to 2.7). We also note that the final point on this curve is markedly less than  $K_r$  and even possibly tends to get smaller than  $K_p$ . It is seen that the RIC current density (curve 2) rises before its maximum as  $t^{0.09}$  and falls afterwards as  $t^{-0.35}$ , close to the law (2).

We measured a current-voltage characteristic (CVC) of both prompt and delayed components using pulsed irradiations 1 ms long (Fig. 4). Unlike previous measurements, both components

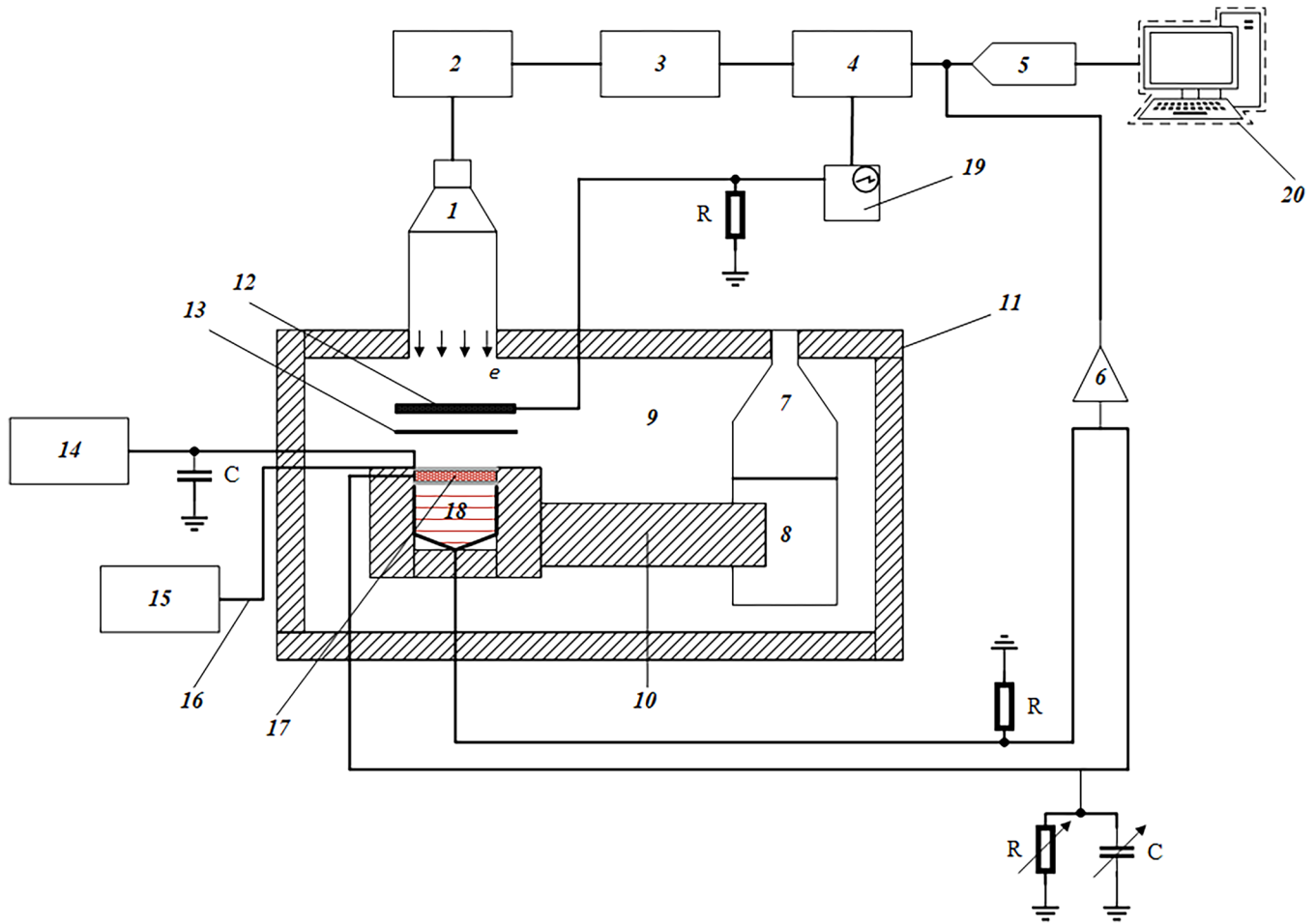


**FIG. 1.** Block diagram of the experimental setup. 1—electron gun; 2—high voltage power supply; 3—modulator; 4—master generator ; 5—analogue-digital converter; 6—amplifier; 7—Dewar’s vessel; 8—liquid nitrogen; 9—vacuum; 10—heat-conducting copper block; 11—vacuum chamber; 12—shutter; 13—polyethyleneterephthalate film; 14—power supply; 15—voltmeter; 16—copper-constantan thermocouple; 17—test PS sample with evaporated electrodes; 18—Faraday cup; 19—oscilloscope; 20—computer for recording and processing experimental data.

could be seen on the same curve like curve 2 in Fig. 2, thus allowing their simultaneous processing.

It is seen from Fig. 4 that CVCs run parallel to each other and in the range of  $10^{(7)-4} \times 10^{(7)}$  V/m the prompt component stays 100 times larger than the delayed one which is measured 10 ms after the pulse end (see curve 2 in Fig. 2).

At fields less than  $2 \times 10^7$  V/m, both curves are roughly linear but in the field range of  $3 \times 10^{(7)-4} \times 10^{(7)}$  V/m for  $j_p$  (for  $j_{rd}$  up to  $6 \times 10^7$  V/m) they become nonlinear  $j \propto F_0^\delta$  with  $\delta \approx 2.0$ . Such CVC behavior is typical for polymers with small delayed component at room temperature.<sup>3</sup> We propose to interpret the above RIC data using the RFV model which was so successful in PS at room temperature.<sup>5</sup> Specific features of the formation of free charge carriers in disordered solids and frozen hydrocarbon glasses at liquid nitrogen temperature will be discussed in due course later.

### III. RFV MODEL AND ITS PARAMETERIZATION

#### A. Model formulation

The basic equations of the RFV model are well-known,<sup>4-6</sup>

$$\begin{cases} \frac{dN(t)}{dt} = g_0 - k_{rec}N_0(t)N(t), \\ \frac{\partial \rho(E, t)}{\partial t} = k_c N_0(t) \left[ \frac{M_0}{E_1} \exp\left(-\frac{E}{E_1}\right) - \rho(E, t) \right] - v_0 \exp\left(-\frac{E}{kT}\right) \rho(E, t), \\ N(t) = N_0(t) + \int_0^\infty \rho(E, t) dE, \end{cases} \quad (3)$$

where  $N_0(t)$  and  $\rho(E, t)$  are both zero at  $t = 0$ .

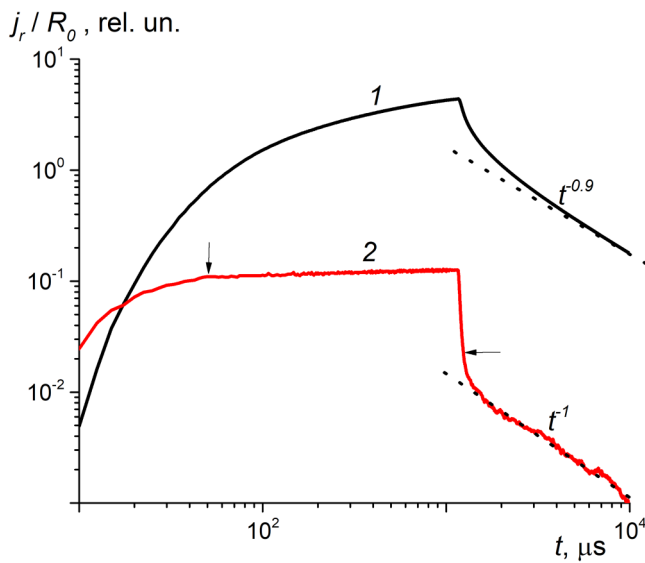


**FIG. 2.** Experimental RIC current transients measured across a 10 kΩ resistor ( $RC < 10 \mu\text{s}$ ) and plotted in logarithmic coordinates. Temperature 290 (1) and 79 K (2), dose rate  $1.3 \times 10^4 \text{ Gy/s}$ . Pulse length: 1 ms, electric field:  $4 \times 10^7 \text{ V/m}$ . The vertical arrow marks the prompt conductivity, the horizontal one—the amplitude of the delayed component at the pulse end.

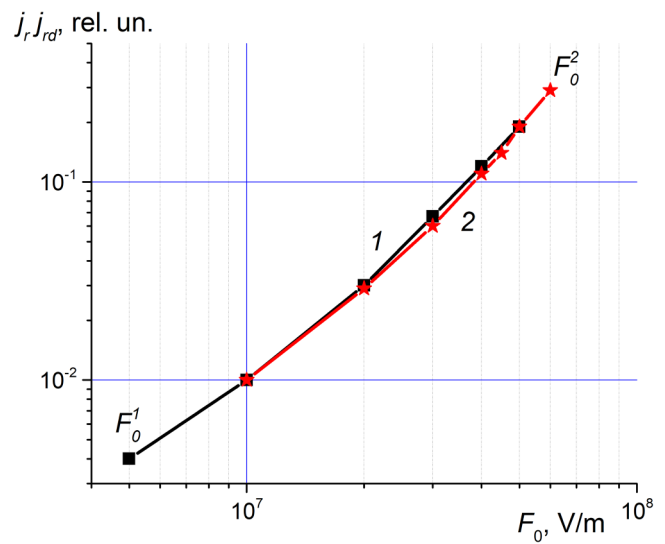


**FIG. 4.** Current–voltage characteristics of the prompt (curve 1, red) and delayed (curve 2, black) RIC components measured at  $t = 0.1 \text{ ms}$  well inside the pulse and at  $t = 10 \text{ ms}$  after its end, respectively (temperature 79 K). Curves 1 and 2 are made to coincide at  $F_0 = 10^7 \text{ V/m}$  (in fact,  $\gamma_p$  is 100 times larger than  $\gamma_{rd}$ ).

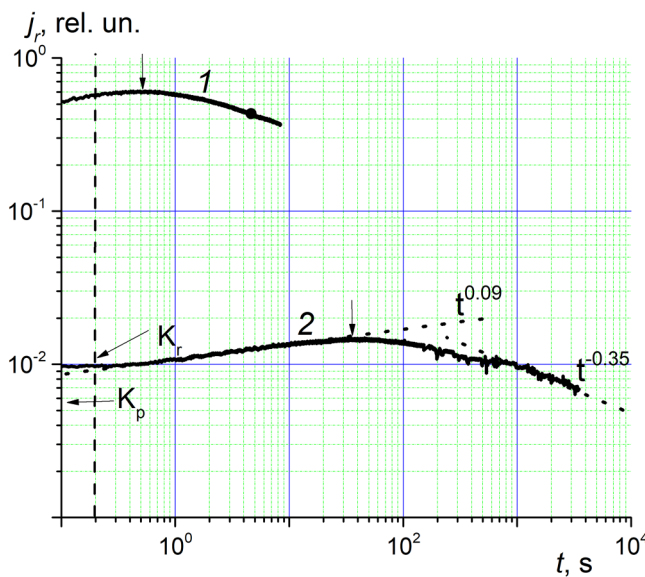


**FIG. 3.** Experimental RIC current transients measured at long-time irradiations and plotted in logarithmic coordinates. Temperature 290 (1) and 79 K (2), dose rate 13 Gy/s. Electric field  $4 \times 10^7 \text{ V/m}$ . The vertical arrows mark the maximum values of the transient curves ( $\gamma_m$ ). Vertical dashed line marks the lower time limit of legitimate RIC measurements (the dead time of the technique).

By definition, the RIC is  $\gamma_r(t) = e\mu_0 N_0(t)$ . Thus, system (2) refers to a unipolar conduction with only one sign carriers being mobile (in our case, holes). The oppositely charged carriers are immobile and act as recombination centers.

Here,  $N(t)$  is the total concentration of radiation-produced holes (due to charge neutrality, equal to that of electrons).  $N_0(t)$  is the concentration of holes in extended states (in the valence band) with the microscopic mobility  $\mu_0$ ;  $g_0$  is the generation rate of free holes (assumed time and space independent during irradiation);  $k_{rec}$  is the recombination coefficient;  $k_c$  is the trapping rate constant;  $M_0$  is the total concentration of traps distributed exponentially in energy  $E$  (taken positive) with the distribution parameter  $E_1$ ;  $\rho(E, t)$  is the time dependent density distribution of trapped holes;  $v_0$  is the frequency factor;  $T$  is the temperature;  $k$  is the Boltzmann's constant, and  $e$  is the elementary electric charge. Also,  $\tau_0 = (k_c M_0)^{-1}$  is the lifetime of mobile holes before trapping. Dispersion parameter  $\alpha = kT/E_1$ .

The second and third equations in system (3) are generic for a quasi-band description of the carrier transport in a dielectric with a unipolar (in our case, hole) conduction. The first equation (the continuity relation) in the present form describes a typical one-dimensional RIC problem ignoring any time-of-flight (TOF) effects. This form of system (3) is used in the present work for identifying RFV parameters.

The RFV model predicts a formal prompt conductivity given by the following formula:<sup>3</sup>

$$\gamma'_p = g_0 \mu_0 \tau_0 e, \quad (4)$$

where  $e$  is an elementary electric charge. To compare it with an

experimental one  $\gamma_p$ , we use reduced quantities  $K_p$  and  $K'_p = \gamma'_p/R_0$ . The general expression relating the carrier generation rate  $g_0$  ( $\text{m}^{-3}\text{s}^{-1}$ ) and the corresponding dose rate  $R_0$  (Gy/s) is as follows:<sup>5</sup>

$$g_0 = 6.24 \times 10^{19} \rho G_{fi} R_0, \quad (5)$$

where  $\rho$  is the polymer density (for PS,  $1.06 \text{ g/cm}^3$ ).

The free ion yield  $G_{fi}$  is defined as  $G_{fi} = G_i f$ , where  $G_i$  means the total yield of geminate pairs (traditionally taken to be equal to 3 per 100 eV of the absorbed energy<sup>5</sup>) and  $f$  is the probability for a pair to escape an initial recombination (the so-called escape probability). In Ref. 5, we used  $G_{fi}$  equal to 1 (at  $4 \times 10^7 \text{ V/m}$  and 290 K) which means that for a dose rate  $1.6 \text{ Gy/s}$ , the carrier generation rate would be  $10^{20} \text{ m}^{-3} \text{ s}^{-1}$ . The escape probability depends on the applied electric field and temperature leading to an appropriate  $K'_p$  variation. Behavior of  $K_p$  is much more stable and it is often even considered as a material parameter.<sup>3</sup> For this reason, comparison of these quantities deserves special attention.

The Onsager theory<sup>7,11,12</sup> of the field-assisted thermal dissociation of the non-interacting electron-hole pairs with an initial distance  $r_0$  between geminate charges in a pair predicts the following field dependence of  $f$  (depicted in Fig. 5). We see that, at high fields ( $>3 \times 10^7 \text{ V/m}$ ),  $f$  does not depend on the temperature for both  $r_0$  chosen (mostly cited in the literature). This fact allows using  $G_{fi}$  equal to unity ( $4 \times 10^7 \text{ V/m}$ , 290 K) as already mentioned.

In Ref. 5, the ratio  $j_{rd}/F_0$  has been employed as an indicator of  $G_{fi}$  because in a small-signal regime and at fields less than  $4 \times 10^7 \text{ V/m}$  (to exclude a possible effect of the rising frequency factor), this quantity is expected to be proportional to the free ion yield. Indeed, under above conditions, the decaying current density  $j_{rd}$  after a pulse end is proportional to  $G_{fi}$ .<sup>5</sup> Experimental data points (open stars) are replotted from Fig. 7 in Ref. 5 and lie closely to the theoretical curve 1 in Fig. 5 confirming the validity of this approach in assessing the functional dependence of  $f(F_0)$ . But to know the absolute value of  $G_{fi}$ , one has to find  $G_{fi}$  at a specific field. According to Hughes,<sup>13</sup> its value in polyvinylcarbazole (PVK), a polymer close to PS by the chemical structure, is about unity at  $4.5 \times 10^7 \text{ V/m}$  and room temperature, thus supporting our choice for this quantity in the present work.

The same approach extended to 79 K (filled stars) in Fig. 5 clearly fails: data points do not follow the theoretical curve 2. In fact, they tend to run close to a theoretical prediction for  $r_0 = 3.5 \text{ nm}$  at room temperature (curve 3) equally contradicting theory for 79 K (curve 4). This unusual result will be discussed below.

## B. Parameterization

In our approach, we assume that all main parameters of the RFV model except  $v_0$  and  $\alpha$  do not change with temperature. Indeed,  $\mu_0$ ,  $\tau_0$ , and  $E_1$  are true microscopic quantities and as such they may be taken to be independent of temperature. As  $\alpha \propto T$  and  $\alpha$  has been taken to be equal to 0.35 at 290 K as in Ref. 2. Then,  $\alpha$  is equal to  $0.35 \times (79/290) = 0.09$  at 79 K.

$f$  and  $j_{rd}/F_0$  (in rel. un.)

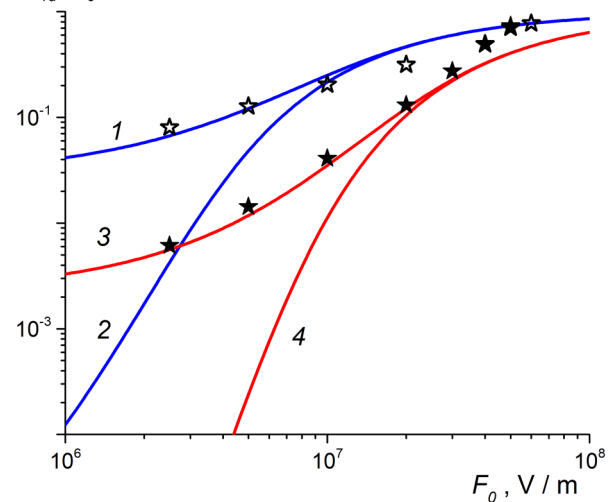


**FIG. 5.** Curves 1–4 describe the field dependence of the surviving probability  $f$  as given by the Onsager theory for  $r_0 = 6 \text{ nm}$  (curves 1 and 2) and  $3.5 \text{ nm}$  (curves 3 and 4) for  $T = 290$  (1, 3) and  $79 \text{ K}$  (2, 4), all given in absolute units. Also, field dependence of the ratio  $j_{rd}/F_0$  (in relative units) obtained at  $79 \text{ K}$  (filled stars) and  $290 \text{ K}$  (open stars), the last replotted from Fig. 7 in Ref. 5. Experimental data are anchored to curve 1 at their highest respective fields.

Repetitive calculations presented in Fig. 6 clearly show that the best fitting value of  $v_0$  is  $4 \times 10^3 \text{ s}^{-1}$  as it reproduces the experimental observation showing that  $\gamma_{rd}$  rises to  $1/5$  of  $\gamma_p$  to the pulse end (points  $a$  and  $b$  on the figure). This value of  $\gamma_{rd}$  persists immediately after the pulse end (point  $d$ ). Curve 5 ( $g_0 = 10^{26} \text{ m}^{-3} \text{ s}^{-1}$ ) exhibits the recombination effect ( $b$  moves to  $c$  and  $d$  to  $e$  reducing by the same factor 1.25). Slopes of decay curves do not change. Some comment is in place. The generation rate used in calculations is  $10^{25} \text{ m}^{-3} \text{ s}^{-1}$  which for  $G_{fi} = 1$  corresponds to  $R_0 = 1.6 \times 10^5 \text{ Gy/s}$  at  $4 \times 10^7 \text{ V/m}$ . As expected, numerical calculations ( $\gamma_p$  at point  $a$  is  $5.6 \times 10^{-10} \Omega^{-1} \text{ m}^{-1}$ ) reproduce an experimental result for  $K_p$  as in Ref. 5.

Now, we should look how well the adopted RFV parameters fit long-time irradiations data (Fig. 7). A group of curves (1–4) illustrates the effect of changing the frequency factor by an order of magnitude which is rather mild similar to what we observed earlier in a pulsed irradiation in Fig. 6.

Current decay after its maximum still under irradiation follows a power law  $\gamma_r \propto t^{-0.43}$  in full accordance with the theoretical prediction  $\gamma_r \propto t^{-(1-\alpha)/2}$  for  $\alpha = 0.09$ .<sup>10</sup> In doing so, the RIC falls well below the reduced prompt conductivity  $K'_p$  observed at times less than a microsecond (Fig. 7). As indicated earlier,  $g_0 = 10^{22} \text{ m}^{-3} \text{ s}^{-1}$  corresponds to  $R_0 = 160 \text{ Gy/s}$  for  $G_{fi} = 1.0$ , which means that  $K'_p = K_p$ . This is an unusual result because a formally defined delayed conductivity  $\gamma_{rd} = \gamma_r - \gamma_p$  gets negative! But this is an intrinsic property of the RFV model. We will consider this situation later in Sec. IV. Also, we see that reducing the generation rate moves the current maximum to longer times in inverse proportion to the generation rate (compare curves 4, 5, and 6 on the figure). Curve 5 in

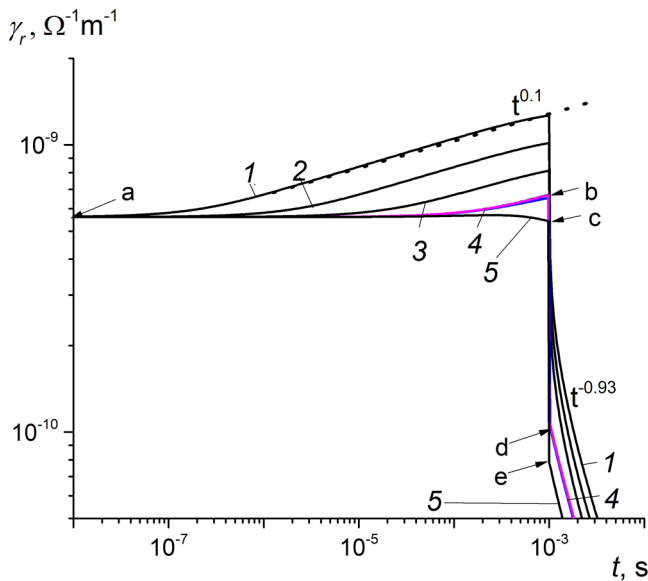


**FIG. 6.** Calculated RIC transients using RFV model parameters given in the first line of Table I except  $\nu_0$  which is a variable. Pulse length 1 ms, carrier generation rate  $10^{25} \text{ m}^{-3} \text{ s}^{-1}$  (curves 1–4) with  $\nu_0$  acting as a parameter equal to  $4 \times 10^6$  (1),  $4 \times 10^5$  (2),  $4 \times 10^4$  (3), and  $4 \times 10^3 \text{ s}^{-1}$  (4, magenta). Curve 4 scales linearly with  $g_0$  up to  $10^{25} \text{ m}^{-3} \text{ s}^{-1}$  but at ten times higher value (curve 5) suffers slight fall approaching the pulse end (to bring it to scale, one has to multiply calculation results by a factor of 10).

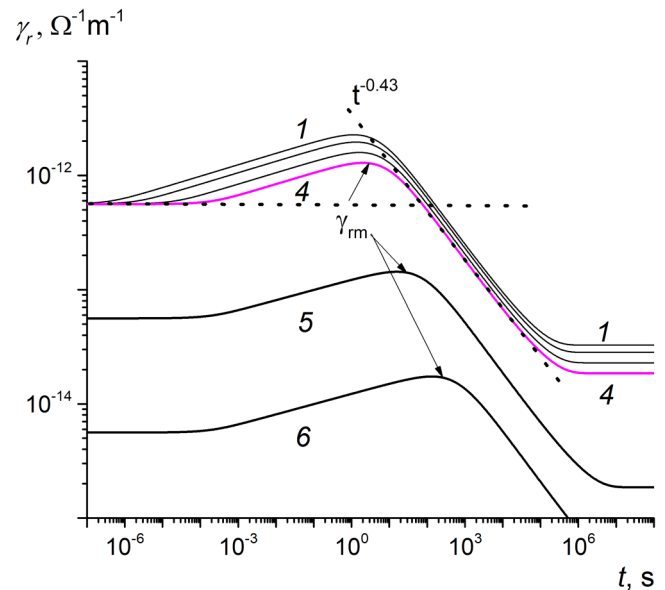


**FIG. 7.** Calculated RIC curves under long-time irradiation using RFV model parameters given in the first line of Table I except  $\nu_0$  which is a variable for an upper group of curves 1–4 (as in Fig. 6). Generation rate  $10^{22}$  (1–4),  $10^{21}$  (5), and  $10^{20} \text{ m}^{-3} \text{ s}^{-1}$  (6). Frequency factor:  $4 \times 10^6$  (1),  $4 \times 10^5$  (2),  $4 \times 10^4$  (3) and  $4 \times 10^3 \text{ s}^{-1}$  [4 (magenta), 5, and 6]. The horizontal dashed line marks the prompt conductivity for curve 4.

Fig. 7 may be used to compare experimental results presented in Fig. 3 with model predictions. Reduced values of  $\gamma_p$  coincide in both cases just as in the case of a pulse irradiation and the ratio  $\gamma_{rm}/\gamma_p$  differ insignificantly (experimental value 2.7 vs simulated 3.0).

Also, current maximum occurs at about 30 s in both cases and it is seen to be roughly proportional to the carrier generation rate. This time increases roughly in reciprocal proportion to decreasing generation rate (compare curves 5 and 6). As expected, decaying currents approach the steady state condition asymptotically decreasing by about 69 times from their maximum values.

Calculations show that  $K_r$  in Fig. 7 is expected to exceed  $K_p$  at  $t = 0.2 \text{ s}$  (dead time in the experiment) by approximately 1.5 times which compares favorably with 1.6 found earlier from Fig. 3. We conclude that RFV parameters given in Table I are quite adequate to describe pulsed and long-time irradiations of PS at 79 K just as those presented in Ref. 5 with proper values of  $\alpha$  and  $\nu_0$  at room temperature.

#### IV. DISCUSSION

##### A. General situation with the RIC in polymers at extremely low temperatures

We have shown that the semi-empirical RFV model in PS at least may be smoothly extended from room and higher temperatures to the liquid nitrogen temperature with only one fundamental amendment concerning the frequency factor  $\nu_0$ . Quite understandably, it had to be drastically reduced. To achieve this, we used a numerical

fitting procedure to a pulsed (1 ms) data corroborated by long-time irradiations as well. No quantitative explanation for this temperature effect could be proposed. The activation energy of the frequency factor in this polymer in a 350–165 K temperature range (0.12 eV) predicts its reduction by a factor of  $8 \times 10^5$  for a temperature change from 290 to 79 K instead of the found value of 2000 only.

This situation is quite intriguing as according to the well-known radiation chemistry results, electrical conduction processes at such extremely low temperatures (about 77 K) are controlled by geminate rather than free charge carriers.<sup>7,8</sup> Indeed, the typical life of an isolated geminate electron-hole pair at a small electric field may be assessed using the following expression:<sup>14</sup>

$$t_g = \nu_0^{-1} \left( \frac{er_c^2}{kT\mu_0\tau_0} \right)^{1/\alpha}, \quad (6)$$

where  $r_c$  (the so-called Onsager radius) is equal to

$$r_c = \frac{e^2}{4\pi\epsilon\epsilon_0kT}. \quad (7)$$

Here,  $\epsilon$  is the relative permittivity (in PS, 2.6) and  $\epsilon_0 = 8.85 \times 10^{-12} \text{ F/m}$  (the dielectric constant). In our case,  $r_c = 22, 4 \text{ nm}$  at 290 K and 82 nm at 79 K. Application of formula (6) shows that  $t_g$  is about 0.01 s (decreasing 10 times at large fields<sup>17</sup>) at room temperature which might explain some peculiarities of the field

**TABLE I.** RFV parameters for PS at  $4 \times 10^7$  V/m for 79 K. Data for  $G_{fi}=2$  are optional (for details, see Ref. 5).

Parameter $G_{fi}$	$\alpha$	$10^5 \mu_0, \text{m}^2/\text{V s}$	$10^{11} \tau_0, \text{s}$	$10^{-3} \nu_0, \text{s}^{-1}$	$10^{14} \kappa_{rec}, \text{m}^{-3} \text{s}^{-1}$
1.0	0.09	1.0	3.5	4	6.9
2.0	0.09	1.0	1.75	4	6.9

dependence in the pulsed RIC in PS at 290 K.<sup>9</sup> At 79 K, this time gets astronomically large.

One of the reviewers raised the question about time-of-flight effects (TOF) in PS at 79 K. In our earlier paper,<sup>5</sup> we specifically discussed TOF effects in PS at room and higher temperatures and showed that the drift hole mobility is very small (even at room temperature it is about  $7 \times 10^{-14} \text{m}^2/\text{V s}$ , see Fig. 5 in Ref. 5). Application of the following formula given in Ref. 4

$$t_{dr} = \nu_0^{-1} \left( \frac{\Gamma(1 + \alpha)L}{\sqrt{6}\mu_0\tau_0 F_0} \right)^{1/\alpha}, \quad (8)$$

where  $L$  is the sample thickness and  $F_0$  is the applied electric field, allows an easy evaluation of the time of flight through a PS film  $20 \mu\text{m}$  thick at  $4 \times 10^7$  V/m which turns to be roughly equal to  $10^{32}$  s. Thus, the drift mobility is so small ( $5 \times 10^{-45} \text{m}^2/\text{V s}$ ) that any TOF effects in PS at 79 K can be safely neglected. Nevertheless, at a semi-empirical level, the multiple trapping approach employed in the RFV model seems to continue to work at this low temperature.

But, the presence of the long-living geminate pairs may still be responsible for the controversy about the field dependence of the ratio  $j_{rd}/F_0$  shown in Fig. 5. At 79 K, there is no reason to expect the formation of free charge carriers with a noticeable probability and one has to associate an explanation of the observed field dependence of the above ratio with intricate laws of the geminate conductivity and recombination.<sup>8</sup>

Now, we would like to discuss the origin of the reduced prompt conductivities  $K_p$  and  $K'_p$  already mentioned in the preceding section. It has been established here and in Ref. 5, that a set of RFV parameters describing the RIC delayed component of PS at room and liquid nitrogen temperatures for both pulsed and long-time irradiations at different fields, allows one to obtain equal values of these two parameters if only at  $4 \times 10^7$  V/m: its value  $3.5 \times 10^{-15} \Omega^{-1} \text{m}^{-1} \text{Gy}^{-1} \text{s}$  according to formulas (4) and (5) corresponds to  $\mu_0\tau_0 = 3.5 \times 10^{-16} \text{m}^2/\text{V}$ . The minimum value of  $\mu_0\tau_0$  found in frozen hydrocarbon glasses at 77 K is 10 times less<sup>8</sup> and was ascribed to the contribution of hot electrons with energies around several eV.

In PS, a polymer with a hopping conduction and in other insulating polymers,  $\mu_0\tau_0$  at 77 K is much higher than its minimum value in a condensed phase. This fact testifies to an overwhelming contribution of the multiple trapping transport through shallow traps in polymers compared with a transport via a long-range tunneling observed in hydrocarbon glasses at these low temperatures. The multiple trapping is still operative at 79 K in PS but the Onsager mechanism of providing holes which are free to move under an applied field clearly fails (see filled stars in Fig. 5). It

should be replaced by the theory of charge carrier generation and current contribution which is yet to be extended from the one-trap systems (hydrocarbon glasses) to polymers with an exponential trap energy distribution. Our effort in this direction is surely to be noted.<sup>14-16</sup>

Concerning curve 2 in Fig. 3, the following should be added. After one hour of continuous irradiation, a reduced current density decreases to  $K_p$  with a clear tendency to fall even further. In view of the above arguments, this is quite possible once recombination time  $t_{rec}$  gets smaller than  $\tau_0$ . The further fall is limited by the above-mentioned minimum of  $\mu_0\tau_0$ . The RIC from that moment would stabilize due to the current contribution by hot electrons insensitive to the bimolecular recombination of thermalized charges. The RFV model does not account for hot electrons and easily admits  $j_{rd}$  falling much lower than  $K'_p$  as Fig. 7 demonstrates (see Ref. 15 where this phenomenon has been reported for  $\alpha \leq 0.1$  even at room temperature). In this situation, the general definition of the RIC delayed component as  $\gamma_{rd} = \gamma_r - \gamma_p$  relates only to a small-signal regime. For the case of the long-time irradiations exceeding a current maximum  $j_m$ , an application of the RFV model needs a special consideration (this problem is typical for extremely low temperatures around 77 K as in our case).

## B. RFV parameter identification

Our previous studies of the RIC in polymers as well as the present investigation show how successful is the RFV model in describing pulsed and long-time irradiations even at 79 K. But one should not forget that it is in principle a semi-empirical model though based on sound physical and chemical processes of radiation interaction with matter. Its main drawback is the non-uniqueness of model parameters as such,<sup>18</sup> but this equally concerns the type of a trap distribution (exponential vs Gaussian).<sup>16,19,20</sup>

Our previous investigations show that both RFV variants with an exponential trap energy distribution (we designated it as MTMe) or with the Gaussian one (MTMg, respectively) are capable to deal with RIC and time-of-flight (TOF) rather successfully giving almost identical results.<sup>19,20</sup> But there is one sticking point concerning the frequency factor in these RFV variants. Its value is typically larger in MMTg by a factor of  $10^4-10^5$ . More to that, we have developed a technique to find  $\nu_0$  directly from a pulsed experiment<sup>21</sup> which was recently used for parameterization of the RFV model in PS.<sup>5</sup> Reported values of  $\nu_0$  (for example, about  $8 \times 10^6 \text{s}^{-1}$  in PS at 290 K as in Ref. 5) and that obtained in the present work ( $4 \times 10^3 \text{s}^{-1}$  at 79 K) are a real challenge to the present-day theory of hopping conduction in disordered solids employing frequency factors around the phonon frequency ( $10^{10}-10^{12} \text{s}^{-1}$ ) as in Refs. 22-24.



Results similar to those presented in Fig. 4 have already been reported for pulse (40 ns) irradiations of polymers at room temperature<sup>21</sup> with some peculiarities at super strong electric fields  $\geq 1.5 \times 10^8$  V/m. At such fields, the frequency factor begins to rise following roughly the Poole–Frenkel law<sup>25</sup> with the growth rate of  $j_{rd}$  exceeding that of  $j_p$  leading to a gross transformation of the current pulse form. Unfortunately, at the present stage, such fields could not be achieved in our laboratory practice.

## V. CONCLUSIONS

It has been shown that the total RIC in PS at 79 K is almost 40 times lower than at room temperature for both pulsed and long-time irradiations. This means that PS being ESD resistant at room temperature should be considered as an ESD prone material at low temperatures (as low as 150 K for sun shaded dielectrics used on the spacecraft outer surfaces). This phenomenon applies equally well to other polymers and should be taken into account in polymer selection for a spacecraft qualification. RIC investigations at low temperatures should be conducted and an appropriate database describing  $\gamma_r(T)$  functional dependence should be provided especially since this dependence is not a simple Arrhenius type with single activation energy.

As far as we know, it is the first detailed investigation of the pulsed and long-time RIC in PS (or any other polymer) at such a low temperature (79 K) that is quite close to the liquid nitrogen boiling temperature 77 K. In these conditions, direct application of the Onsager theory<sup>11,12</sup> is problematic. But, we have shown that RIC even at 79 K can be satisfactorily described by the semi-empirical RFV model based on the quasi-band multiple trapping mechanism<sup>26,27</sup> provided that two model parameters ( $\alpha$  and  $\nu_0$ ) are properly changed by numerically fitting experimental data (in our case,  $\alpha = 0.09$  and  $\nu_0 = 4 \times 10^3 \text{ s}^{-1}$  at 79 K). But prompt and delayed components of the RIC at fields exceeding  $2 \times 10^7$  V/m exhibit a non-linear behavior in a very similar manner.

Parameter  $K_p = 3.5 \times 10^{-15} \Omega^{-1} \text{ m}^{-1} \text{ Gy}^{-1} \text{ s}$  ( $\pm 20\%$ ) at  $4 \times 10^7$  V/m and is independent of temperature (290 or 79 K). The field dependence of the ratio  $j_{rd}/F_0$  measured in a small-signal regime which was a useful indicator of the free ion yield at 290 K (see Ref. 5) but at 79 K this approach clearly fails (as Fig. 5 shows). We believe that this is due to the predominant presence of geminate electron–hole pairs. An adequate accounting of their presence needs a more detailed and complicated analysis based on radiation chemistry results.<sup>7,8</sup> Parameter values of the RFV model for PS at 79 K are given in Table I.

## ACKNOWLEDGMENTS

The authors are indebted to the Basic Research Program of the National Research University Higher School of Economics, Moscow, for their support.

## AUTHOR DECLARATIONS

### Conflict of Interest

The authors have no conflicts to disclose.

## Author Contributions

**Andrey Tyutnev:** Conceptualization (equal); Investigation (equal); Supervision (equal). **Vladimir Saenko:** Investigation (equal); Methodology (equal). **Ilshat Mullakhmetov:** Investigation (equal); Methodology (equal); Software (equal). **Andrey Abrameshin:** Conceptualization (equal); Resources (equal); Supervision (equal).

## DATA AVAILABILITY

The data that support the findings of this study are available from the corresponding author upon reasonable request.

## REFERENCES

- H. B. Garrett and A. C. Whittlesey, *Guide to Mitigating Spacecraft Charging Effects* (Wiley, New York, 2012).
- B. Gross, “Radiation induced charge storage and polarization,” in *Electrets*, edited by G. M. Sessler (Springer-Verlag, New York, 1980).
- A. Tyutnev, V. Saenko, E. Pozhidaev, and R. Ikhsanov, *IEEE Trans. Plasma Sci.* **43**, 2915 (2015).
- A. Tyutnev, V. Saenko, R. Ikhsanov, and E. Krouk, *J. Appl. Phys.* **126**, 095501 (2019).
- A. Tyutnev, V. Saenko, I. Mullakhmetov, and I. Agapov, *J. Appl. Phys.* **129**, 175107 (2021).
- G. S. Mingaleev, A. P. Tyutnev, B. P. Gerasimov, and I. A. Kulchitskaya, *Phys. Status Solidi A* **93**, 251 (1986).
- G. R. Freeman, *Kinetics of Non-Homogeneous Processes* (Wiley, New York, 1987).
- B. S. Yakovlev and L. V. Lukin, *Adv. Chem. Phys.* **60**, 99 (1985).
- A. P. Tyutnev, D. N. Sadovnichii, V. S. Saenko, and E. D. Pozhidaev, *Polym. Sci. A* **47**, 1174 (2005).
- V. I. Arkhipov, J. A. Popova, and A. I. Rudenko, *Philos. Mag. B* **48**, 401 (1983).
- L. Onsager, *Phys. Rev.* **54**, 554 (1938).
- K. M. Hong and J. Noolandi, *J. Chem. Phys.* **69**, 5026 (1978).
- R. C. Hughes, *IEEE Trans. Nucl. Sci.* **18**, 281 (1971).
- A. P. Tyutnev, V. R. Nikitenko, V. S. Saenko, and E. D. Pozhidaev, *Khim. Fizika* **19**, 90 (2000) (in Russian).
- A. P. Tyutnev, *High Energy Chem.* **30**, 1 (1996).
- A. P. Tyutnev, D. S. Weiss, D. H. Dunlap, and V. S. Saenko, *J. Phys. Chem. C* **118**, 5150 (2014).
- T. Chandrasekaran and J. Silverman, *J. Chem. Phys.* **66**, 1786 (1977).
- A. P. Tyutnev, V. S. Saenko, E. D. Pozhidaev, and V. A. Kolesnikov, *J. Phys.: Condens. Matter* **18**, 6365 (2006).
- A. Tyutnev, V. Saenko, and E. Pozhidaev, *Chem. Phys.* **415**, 133 (2013).
- A. P. Tyutnev, V. R. Nikitenko, V. S. Saenko, and E. D. Pozhidaev, *Russ. J. Phys. Chem. B* **1**, 661 (2007).
- A. P. Tyutnev, V. N. Abramov, P. I. Dubenskov, V. S. Saenko, A. V. Vannikov, and E. D. Pozhidaev, *Acta Polym.* **37**, 336 (1986).
- H. Bäessler, *Phys. Status Solidi B* **175**, 15 (1993).
- P. M. Borsenberger and D. S. Weiss, *Organic Photoreceptors for Imaging Systems* (Marcel Dekker, New York, 1993).
- S. D. Baranovskii, *Phys. Status Solidi A* **215**, 1700676 (2018).
- A. P. Tyutnev, B. L. Linetskii, A. V. Nikerov, and V. S. Saenko, *Russ. J. Phys. Chem. B* **9**, 648 (2015).
- J. Noolandi, *Phys. Rev. B* **16**, 4466 (1977).
- T. Tiedje and A. Rose, *Solid State Commun.* **37**, 49 (1981).